Supplementary Materials

Co single atoms/nanoparticles over carbon nanotubes for synergistic oxidation of 5-hydroxymethylfurfural to 2,5-furandicarboxylic acid

Chengfeng Yi, Zhigang Liu*

Advanced Catalytic Engineering Research Center of the Ministry of Education, College of Chemistry and Chemical Engineering, Hunan University, Changsha 410082, Hunan, China.

***Correspondence to:** Prof. Zhigang Liu, College of Chemistry and Chemical Engineering, Hunan University, Lushan South Road No.2, Changsha 410082, Hunan, China. E-mail: liuzhigang@hnu.edu.cn

Characterization

Sample characteristics were determined using various analytical techniques. The specific surface area and pore size distribution were calculated using the Brunauer-Emmett-Teller (BET) and Barrett-Joyner-Halenda (BJH) methods, respectively. The samples were degassed under vacuum at 200 ℃ for 2 h before analysis using a JW-BK200C apparatus. The crystal structures of the samples were examined through Powder X-ray diffraction (XRD) using a Bruker D8 Advance X-ray diffractometer with Cu Kα radiation (40 kV). Raman analysis was conducted on a Witec Alpha300R Spectrometer with a 633 nm laser. For morphological and compositional characterization, transmission electron microscopy (TEM) was performed using the Themis Z (3.2) instrument, and scanning electron microscopy (SEM) was carried out using the S-4800 instrument from Japan HITACHI. X-ray photoelectron spectroscopy (XPS) was conducted on a Thermo Fisher ESCALAB Xi+ X-ray photoelectron spectrometer with Al Kα radiation (hv = 1486.6 eV). The cobalt content in the samples was determined using an Agilent 7800 inductively coupled plasma spectrometer (ICP-MS). H_2-temperature programmed reduction (H_2-TPR) analysis was performed on a dynamic adsorption instrument from Huasi. A quartz tube containing 25.0 mg of the sample was pre-treated at 200 °C under N_2 atmosphere for 30 minutes and then cooled to room temperature. Subsequently, the sample was exposed to the 5% H_2/N_2 atmosphere and heated at the rate of 10 °C min^{-1} up to 600 °C. The reduction of cobalt species was monitored using a thermal conductivity detector (TCD).

Data reduction, data analysis, and extended X-ray absorption fine structure (EXAFS) fitting were performed and analyzed with the Athena and Artemis programs of the Demeter data analysis packages that utilizes the FEFF6 program to fit the EXAFS data. The energy calibration of the sample was conducted through standard and Co foil, which as a reference was simultaneously measured. A linear function was subtracted from the pre-edge region, then the edge jump was normalized using Athena software. The χ(k) data were isolated by subtracting a smooth, third-order polynomial approximating the absorption background of an isolated atom. The k^3-weighted χ(k) data were Fourier transformed after applying a HanFeng window function (Δk = 1.0). For EXAFS modeling. The global amplitude EXAFS (CN, R, σ^2 and ΔE_0) were obtained by nonlinear fitting, with least-squares refinement, of the EXAFS equation

to the Fourier-transformed data in R-space, using Artemis software, EXAFS of the Co foil are fitted and the obtained amplitude reduction factor $S\sigma^2$ value (0.708) was set in the EXAFS analysis to determine the coordination numbers (CNs) in sample. For Wavelet Transform analysis, the $\chi(k)$ exported from Athena was imported into the Hama Fortran code. The parameters were listed as follow: R range, 1.0-4.0 Å, k range, 0-12.0 $Å^{-1}$; k weight, 3; and Morlet function with $\kappa = 15$, $\sigma = 1$ was used as the mother wavelet to provide the overall distribution.

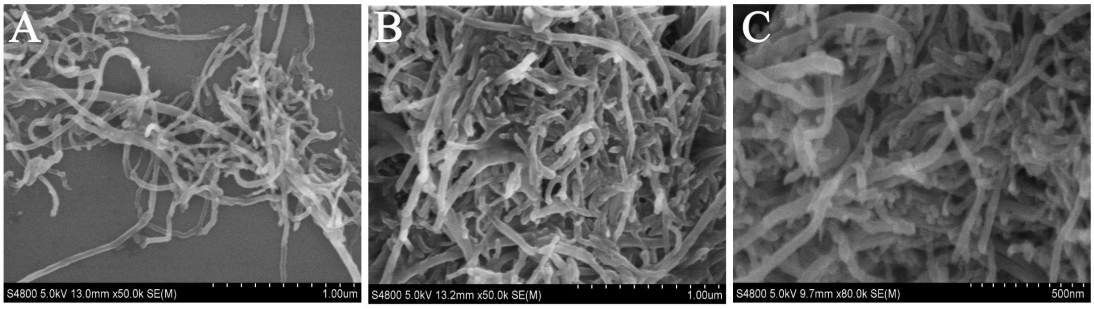

Supplementary Figure 1. SEM images of (A) CNTs, (B) Co@CNTs and (C) Co SAs/NPs@N-CNTs.

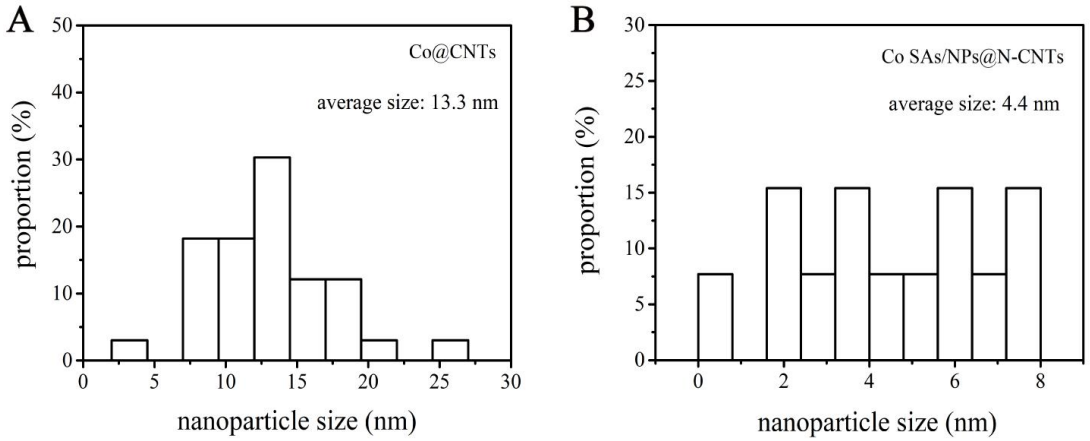

Supplementary Figure 2. The metal nanoparticle size distribution of (A) Co@CNTs and (B) Co SAs/NPs@N-CNTs.

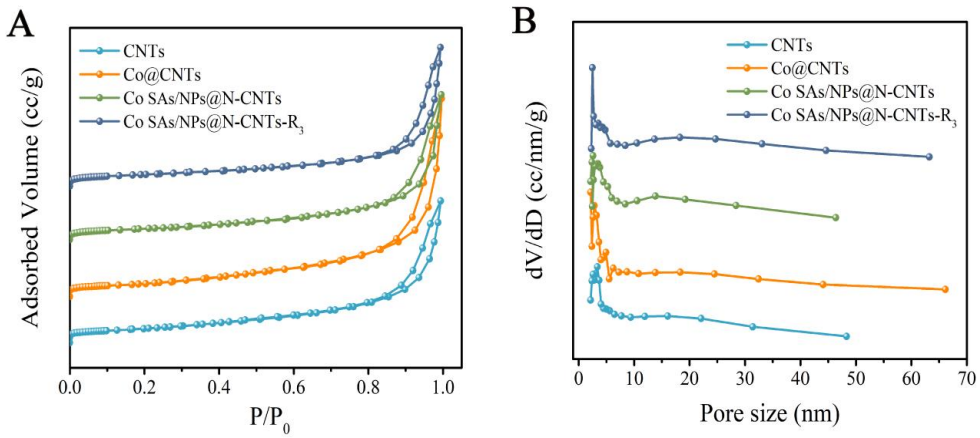

Supplementary Figure 3. (A) N_2 adsorption-desorption isotherms and (B) pore size distribution of CNTs, Co@CNTs, Co SAs/NPs@N-CNTs and Co SAs/NPs@N-CNTs-R_3.

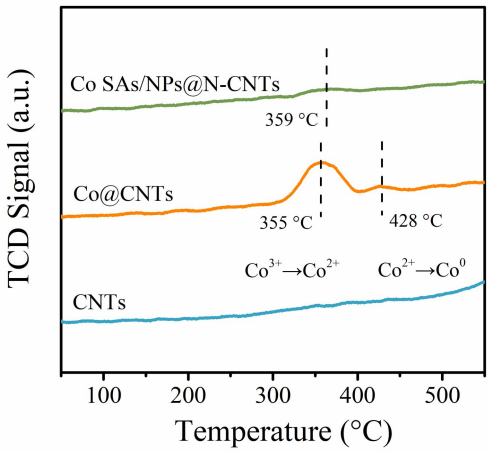

Supplementary Figure 4. H_2-TPR curves of CNTs, Co@CNTs and Co SAs/NPs@N-CNTs.

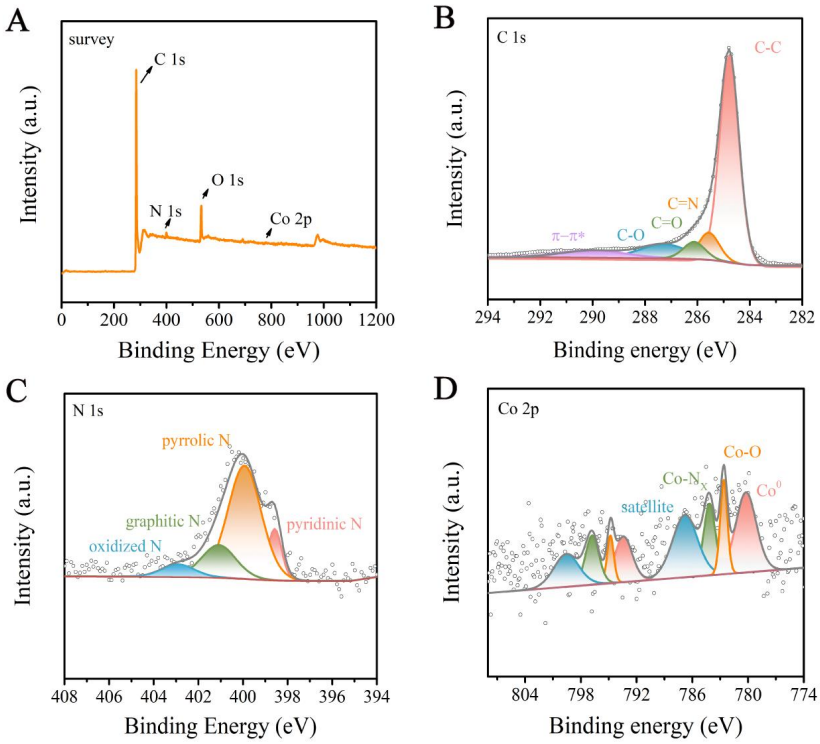

Supplementary Figure 5. (A) XPS full spectra, high-resolution XPS spectrum for (B) C 1s, (C) N 1s and (D) Co 2p of Co SAs/NPs@N-CNTs-R_3.

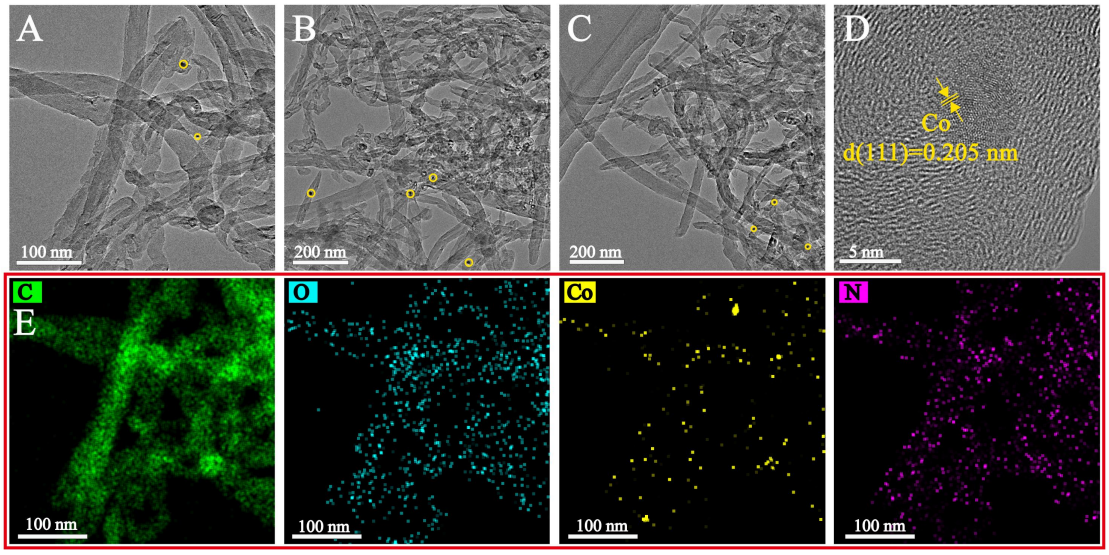

Supplementary Figure 6. (A-C) TEM images of Co-N@CNTs-R_3 under different vision, (D) HR-TEM image of Co SAs/NPs@N-CNTs-R_3, (E) HAADF-STEM image and corresponding element mappings of Co SAs/NPs@N-CNTs-R_3 for C, O, Co, N.

Supplementary Table 1. Porosity parameters of CNTs, Co@CNTs, Co SAs/NPs@N-CNTs and Co SAs/NPs@N-CNTs-R_3

Sample	S_{BET} ($m^2 \cdot g^{-1}$)	V_{total} ($cm^3 \cdot g^{-1}$)	D_p (nm)
CNTs	87	0.40	18.40
Co@CNTs	82	0.38	18.05
Co SAs/NPs@N-CNTs	79	0.41	23.74
Co SAs/NPs@N-CNTs -R_3[a]	75	0.40	21.13

[a]Co SAs/NPs@N-CNTs after three repeated experiments.

Supplementary Table 2. Elemental analysis based on XPS spectra

Sample	C (%)	O (%)	N (%)				
			Total	Pyridinic N	Pyrrolic N	Graphitic N	Oxided N
Co@CNTs	97.4	2.3	-	-	-	-	-
Co SAs/NPs@ N-CNTs	92.1	4.1	3.3	48.0	27.5	13.5	11.0
Co SAs/NPs@ N-CNTs -R_3	89.5	8.0	2.4	11.8	62.9	18.5	6.8

Sample	Co (%)			
	Total	Co^0	Co-O	Co-N_X
Co@CNTs	0.3	43.3	56.6	-
Co SAs/NPs@N-CNTs	0.5	49.9	25.3	24.8
Co SAs/NPs@N-CNTs -R_3	0.2	51.3	20.7	28.0

Supplementary Table 3. EXAFS fitting parameters at the Co K-edge for various samples (S_0^2 = 0.911)

Sample	Shell	CN^a	R(Å)^b	σ^2(Å^2)^c	ΔE_0(eV)^d	R factor
Co foil	Co-Co	12*	2.49 ± 0.01	0.0063	7.2	0.0014
CoPc	Co-N	4.1±0.2	1.90 ± 0.01	0.0014	11.7	0.0098
Co SAs/NPs	Co-N	2.4±0.4	1.91 ± 0.01	0.0051	2.1	0.0116
@N-CNTs	Co-Co	4.6±0.5	2.49 ± 0.01	0.0066	7.5	

[a]*CN*, coordination number; [b]*R*, distance between absorber and backscatter atoms; [c]σ^2, Debye-Waller factor to account for both thermal and structural disorders; [d]ΔE_0, inner potential correction; *R* factor indicates the goodness of the fit. S_0^2 was fixed to 0.708, according to the experimental EXAFS fit of Co foil by fixing CN as the known crystallographic value. A reasonable range of EXAFS fitting parameters: $0.600 < S_0^2 < 1.000$; $CN > 0$; $\sigma^2 > 0$ Å^2; $|\Delta E_0| < 15$ eV; *R* factor < 0.02.

Supplementary Table 4. The selective oxidation of HMF on different catalysts

Sample	Conversion (%)	Yield (%)				Total yield (%)
	HMF	FDCA	FFCA	DFF	HMFCA	
-	94.2	13.7	39.2	5.1	15.4	73.4
CNTs	91.9	12.4	35.8	7.2	15.5	70.9
Co@CNTs	97.7	23.0	39.8	3.4	18.1	84.3
Co SAs/NPs@N-CNTs	100.0	94.2	4.0	0.4	0.0	98.6
Co SAs@N-CNTs	99.9	92.2	5.8	0.9	0.0	98.9
Co NPs@N-CNTs	99.7	44.4	32.5	2.6	3.3	82.8
N-CNT	99.2	46.0	33.1	2.9	2.7	84.6

Reaction condition: catalyst (20 mg), HMF (0.1 mmol), TBHP (1.68 mL), DMSO (5mL), 80 °C, 24 h.

Supplementary Table 5. Reaction rate constant of the oxidation of (a) DFF and (b) FFCA over Co SAs/NPs@N-CNTs and Co SAs@N-CNTs at 80 °C

Sample	K_{DFF} (min^{-1})	K_{FFCA} (min^{-1})
Co SAs/NPs@N-CNTs	0.02109	0.01727
Co SAs@N-CNTs	0.01348	0.01174

Supplementary Table 6. The recyclability of Co SAs/NPs@N-CNTs for the selective oxidation of HMF

Sample	Conversion (%)	Yield (%)				Total yield (%)
	HMF	FDCA	FFCA	DFF	HMFCA	
Co SAs/NPs@N-CNTs	100.0	94.2	4.0	0.4	0.0	98.6
Co SAs/NPs@N-CNTs-R_1[a]	100.0	40.5	40.0	2.1	7.5	90.1
Co SAs/NPs@N-CNTs-R_2[b]	98.6	31.3	41.6	4.8	12.3	90.0
Co SAs/NPs@N-CNTs-R_3[c]	96.0	22.8	42.7	6.2	16.2	87.9
Co SAs/NPs@N-CNTs-R_3 -600 °C[d]	98.2	29.4	44.4	5.0	14.3	93.1

Reaction condition: catalyst (20 mg), HMF (0.1 mmol), TBHP (1.68 mL), DMSO (5 mL), 80 °C, 24 h. [a]the catalyst after one repeated experiments; [b]the catalyst after two repeated experiments; [c]the catalyst after three repeated experiments; [d]the catalyst after three repeated experiments calcined at 600 °C in N_2 atmosphere.